

Block copolymer micelles, micellar networks and mesophases

K. Mortensen

Condensed Matter Physics and Chemistry Department, Risø National Laboratory, DK-4000 Roskilde, Denmark.
E-mail: kell.mortensen@risoe.dk

Block copolymers aggregate in selective solvents into micelles of various form and size depending on molecular architecture and interaction parameters. The micelles constitute the basis for a variety of novel mesophases, including bicontinuous phases and networks of ordered micelles. Small-angle scattering of X-rays and neutrons are among the most central tools to investigate the structural properties, and thereby thermodynamics and dynamics of such complex block copolymer micellar systems.

Introduction

The physical properties of amphiphilic macromolecules constitute a rich topic which in recent years has attracted interest within both applied and basic science [1-7].

When block-copolymers are mixed in a solvent which dissolves only one of the blocks, the molecules self-associate into specific structures to avoid direct contact between solvent and the blocks which are insoluble. This self-association gives rise to a wide range of phase behavior, including the formation of micelles of various form and size,

complex structured microemulsions, and liquid crystalline phases. A variety of block copolymers, have in this context been studied when dissolved in selective solvents of both polar and non-polar type. In aqueous systems, particular interests have concerned block copolymers based on poly(ethylene oxide), PEO, as the water soluble block.

Block copolymer self-association into micellar aggregates

It is well established that di- and triblock copolymers of AB or ABA type, respectively, typically form micellar aggregates in solvents which are thermodynamically good for the A-block and precipitants for the B-block. Such micelles constitute a liquid suspension of hard sphere interacting units, as illustrated in Figure 1a. Triblock copolymers of BAB architectures may also form individual micelles, but this implies that all polymer chains start and end in the same micelle having the middle A-block dispersed into the liquid, the so-called flower type micelles. More likely, such micelles form interconnected networks, where cores are connected by the soluble A-polymer block, as shown schematically in Figure 1b and c.

Critical micellization temperature and concentration

In general, micellization of block copolymers assumes equilibrium between molecularly dispersed copolymers (unimers) and multi-molecular aggregates (micelles). Aqueous systems of block

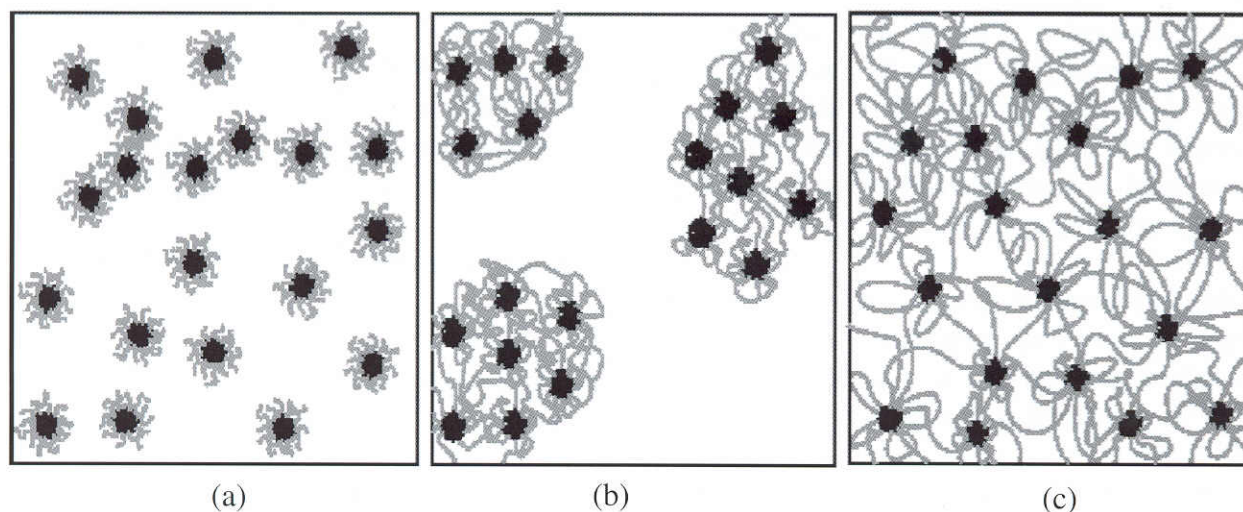


Figure 1: Schematic representation of spherical micelles. (a) Micelles of AB or ABA type of block copolymers, resulting in independent hard-sphere interacting aggregates. (b) and (c) Micelles of BAB type of block copolymers, resulting in domains of interconnected networks of spherical aggregates.

copolymer composed of PEO with either PPO or PBO constitute very good model systems for studying the micellization process and micellar interactions. At low temperature all these polymers are hydrophilic, while at higher temperatures PPO and PBO become hydrophobic.

PEO-PPO-PEO and PEO-PBO-PEO copolymers therefore appear as unimers when mixed with water at low temperatures. Structural studies based on neutron scattering [5] indicate, however, that the unimers have the form of uni-molecular micelles presumably with the PPO-blocks at the centre, rather than Gaussian chains. The temperature-induced change in hydrophobicity leads to a temperature above which micellar aggregates are formed with a core dominated by PPO (respectively PBO) and surrounded by a corona of hydrated PEO sub-chains. Depending on the molecular architecture and the interaction parameters, various micellar forms can appear, including spherical, rod-like and disc shaped. In the PEO-PPO-PEO-systems, thermodynamic changes from spherical to rod-like, discs and possibly bicontinuous microemulsion [8] can be induced by changing temperature or concentration.

Typical scattering functions of $\text{EO}_{99}\text{PO}_{65}\text{EO}_{99}$ -micelles are shown in Figure 2 [9]. The characteristics of the scattering functions are the concentration-dependent correlation hole at low- q (q being the scattering vector), the side maximum near $q=0.1\text{\AA}^{-1}$ and the limiting $I\sim q^{-2}$ behavior at high q -values, reflecting to first order respectively the inter-micellar correlations, the micellar core and the dispersed PEO-chains.

The micellar form factor can be expressed analytically assuming a dense core and Gaussian chains in the corona [10]. The solid lines in Figure 2 represent best fits to this formula, including instrumental smearing and inter-micellar correlations based on hard sphere interactions in the Percus-Yevick approximations [11].

The spherical micellar conformations have been confirmed by direct imaging, using cryo-TEM [9]. The micellar characteristics as obtained from SANS may also be compared to the hydrodynamic radius, R_h , as obtained using dynamic light scattering [12,13]. Generally, the hydrodynamic radius is larger than the core and smaller than the interaction-radius.

One of the important parameters obtained from the

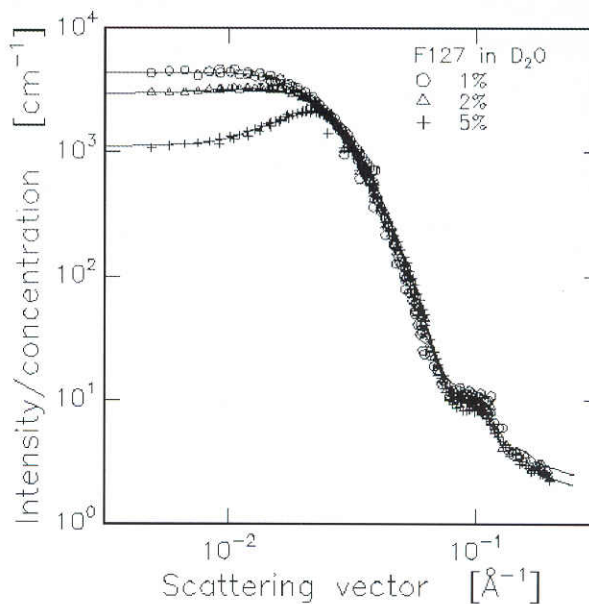


Figure 2: Examples of scattering functions, $I(q)$, of different concentrations of spherical ABA triblock copolymer micelles ($\text{EO}_{97}\text{PO}_{65}\text{EO}_{97}$) obtained at $T=35^\circ\text{C}$. The solid lines represent the best fit of micellar form factor and structure factor with a hard-sphere interacting potential.

experimental scattering data and other indirect techniques is the micellar volume fraction, ϕ . Figure 3 shows a contour plot of ϕ -data of $\text{EO}_{25}\text{PO}_{40}\text{EO}_{25}$ [5,14]. The variation in ϕ separates into four regimes. At low temperatures and concentrations, all polymers are dissolved as the unimers. Above a line of critical micellization temperatures ($T_{\text{cm}1}$) and concentrations (cmc_1), a regime of coexisting micelles and unimers appears. The dispersion is totally dominated by micelles in the regime above $T\sim 30^\circ\text{C}$. For copolymer concentration more than approximately 20%, the micelle volume fraction reaches a limiting value of the order of $\phi_c \sim 0.53$. On crossing this $\phi_c \sim 0.53$ line, the suspension undergoes a transition from a low- T / low-concentration liquid to a high- T / high-concentration solid.

Micellar Size and Aggregation Number

The micellar core-radius, R_c , of PEO-PPO-PEO copolymers is roughly independent of copolymer concentration, but shows temperature dependence reflecting changes in aggregation number [5,15]. The change in micellar radius for different PEO-PPO-PEO copolymers shows very similar characteristics. The core size follows an empirical scaling relation

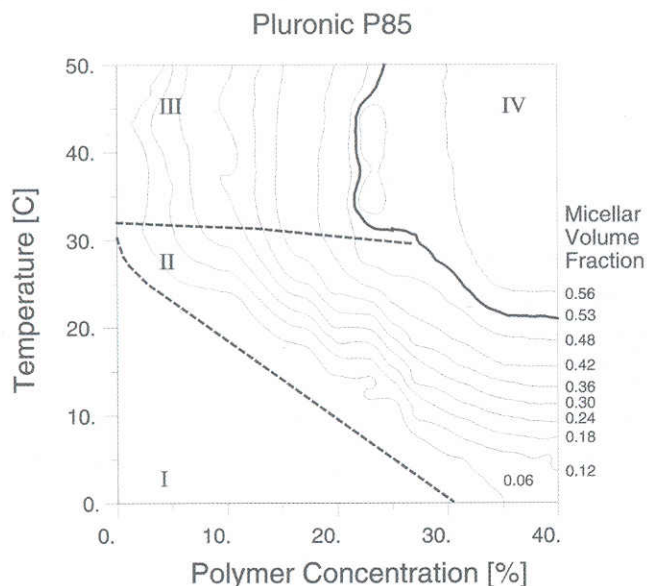


Figure 3: Temperature/polymer-concentration contour plot showing the experimental micellar volume fraction ϕ of aqueous solutions of $\text{EO}_{97}\text{PO}_{65}\text{EO}_{97}$. The solid line represents $\phi=0.53$ separating the micellar liquid and cubic ordered phase. The other lines are guides separating the characteristic regimes of pure unimers (phase I); unimers + micelles (phase II); and spherical micelles (phase III (liquid) and phase IV (solid)).

relative to the reduced temperature: $R_c \sim (T - T_{cm1})^{0.2}$. The aggregation number N_{agg} can be calculated both from the core dimension and, independently of, based on the limiting micellar volume fraction, with very good agreement [16]. The values range from less than 10 to more than 200, depending on temperature.

Rod and worm-like micelles

Depending on the block copolymer design and depending on the specific interaction parameters

between solvent and polymer blocks, other forms than spherical aggregates may occur. In the $\text{EO}_m\text{PO}_n\text{EO}_m$ -copolymers it is possible thermodynamically to follow such transitions from spherical to rod and disc shapes by changing the temperature and/or changing the size of the PEO-blocks. At elevated temperatures, aqueous solutions of PEO-PPO-PEO show form-transformation from sphere to rod-like micelles [5,15]. The origin of the sphere-to-rod transition is related to the size of the spherical aggregates. Close to the sphere-to-rod transition the core-radius is large relative to the polymer backbone, resulting in either highly stretched PPO-chains, or major mixing of EO and PO inside the core, which respectively is entropically costly and causes an increase in chemical potential [5,15].

The rod-like micelles form potentially a nematic phase above some concentration limits. In steady shear it was shown that the PEO-PPO-PEO rod-like micelles align to various degrees depending on polymer concentration and shear-rate, as shown in Figure 4 [5,14].

Cubic phase of spherical ABA and AB block copolymer micelles

In the contour plot of the micellar volume fraction, ϕ , shown in Figure 3, we see that ϕ saturates at a limiting value of the order of $\phi_c=0.53$. When the ϕ_c border-line is crossed the micellar liquid undergoes a first order phase transition to a cubic crystal [17,18], in agreement with simple hard-sphere crystallization. Both bcc [5,14] and fcc [19] phases have been reported in the PEO-PPO-PEO and related micellar systems [20].

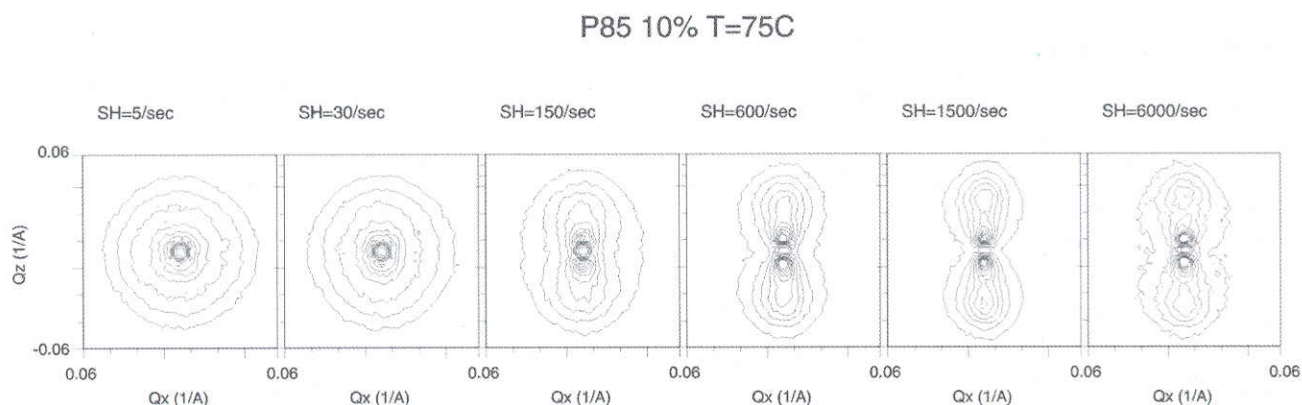


Figure 4: Shear induced alignment of rod-like micelles into a nematic state.

Shear has a marked effect on the cubic crystalline texture, but seems to depend critically on the specific copolymer architecture. While original studies showed only minor shear dependence [5], more recent experiments have shown shear thinning and structural dislocation [21-23] analogous to the results of Gast and coworkers on PS-PI [20]. In static flow conditions, the shear aligned texture of bcc-crystals is most often found corresponding to a mono-domain with $q_v \parallel [112]$ and $q_\nabla \parallel [111]$, where q_v and q_∇ are the q -vector parallel to shear flow and shear gradient, respectively. In large amplitude oscillatory shear, on the other hand, the texture is usually a twin structure with $q_v \parallel [111]$ and $q_\nabla \parallel [110]$.

The mono-domain cubic phase of PEO-PPO-PEO micelles typically has a mosaicity of the order of 10° [5,24]. With shear-oriented crystals, it is possible to perform crystallographic studies and indexing of the observed Bragg-reflections [5,24]. In Figure 5 is shown the two-dimensional scattering pattern of $EO_{96}PO_{39}EO_{96}$ with the beam along the shear gradient and when the sample is rotated 35° around the primary [110]-reflection. The scattering pattern is in agreement with a bcc-lattice, as indicated by the associated Miller indices.

In the limit of high temperature and/or high polymer concentration, the cubic phase of the $EO_mPO_nEO_m$ micelles melts near the transition from a spherical to a rod-like form.

Micelles with glassy cores.

A number of micelles are composed of block copolymers where the non-soluble block is a glass at relevant temperatures. Any dynamics involving molecules jumping from one micelle to another or micellar shape transformations are frozen out. Block copolymers of PS are examples of such systems. Mixing PS-PEO block copolymers with water at ambient temperatures leads to large plate or rod-like micelles given by the original lamellar sheets of the bulk PS-PEO. Only when annealed above the glass transition of the PS-block do the micelles relax to the spherical equilibrium structure [25]. In triblock copolymers of the BAB type, the glassy cores have a particularly strong influence, since these make up a permanent physical network structure.

BAB block copolymer architecture

The phase behavior of the BAB-type of triblock copolymer in a solvent selective for the mid-block, is to form quite different structures relative to the AB and ABA types. These polymers may also form micellar aggregates. Frequently, however, the dilute-concentration causes loose structures of less well defined aggregates [7,26].

In the micellar phase, the A-midblocks of the BAB copolymers form either loops or bridges between micelles. The inter-micellar bridging gives rise to

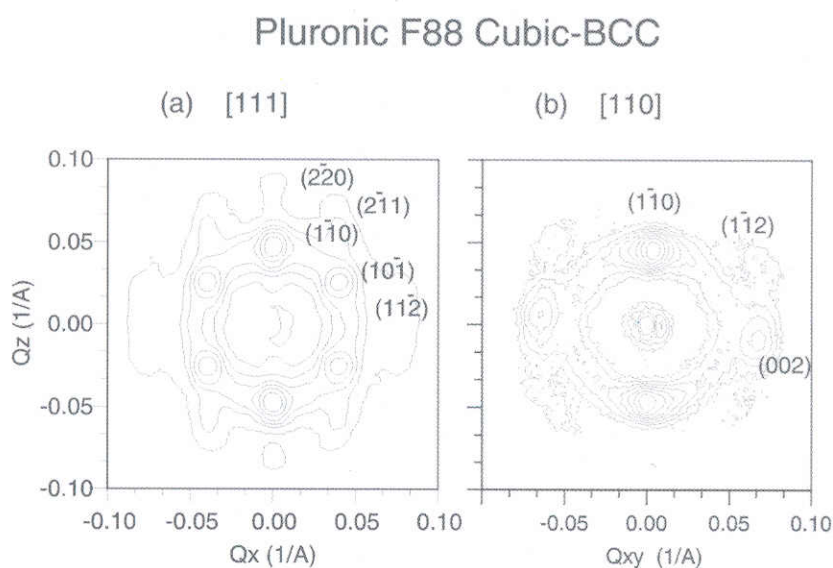


Figure 5: Two dimensional scattering function of $EO_{96}PO_{40}EO_{96}$, (a) as obtained with the shear axis parallel to the beam, and (b) as observed when the sample is rotated by 35° around the vertical axis.

clusters of highly interconnected micelles. For a certain copolymer concentration, the micellar networks extend over the whole sample volume, thus providing a macroscopically isotropic physical gel. In $PO_nEO_mPO_n$ and $BO_nEO_mBO_n$ -systems, cubic ordered structure is observed in the isotropic phase at low temperatures [26-30].

The usual Pluronics, $EO_mPO_nEO_m$, might be of the BAB-type if dispersed in nonpolar solvents. Alexandridis and coworkers and Chu and coworkers have studied the aggregation behavior of $EO_mPO_nEO_m$ in xylene and found micelles with predominantly individual flower type micelles [31-34].

Micellar networks

Depending on the lifetime of the polymer blocks associated to a given core, BAB-material may show a finite elastic response. Systems with glassy micellar cores are ideal systems for such elastomers crosslinked by self-association. A number of studies have focused on the PS-type of block copolymers, including PS-PI-PS [35,36], PS-PEP-PS [37] and PS-PEB-PS [38,39]. Scattering experiments as well as electron microscopy imaging have clearly revealed the spherical PS-cores with effectively hard-sphere interaction.

The microscopic response to macroscopic deformation of the three-dimensional network was studied by neutron scattering. Upon stretching up to about 100%, additional correlations appear in specific directions, resembling induced paracrystalline order, as shown in Figure 6 [40]. Further stretching gives rise to an anisotropic pattern of the butterfly type, indicating non-homogeneous connectivity [41].

Shear alignment of BAB copolymer ordered networks

For polymer concentrations of 15% or more, ordered cubic structures are observed above $T \approx 55^\circ\text{C}$ [42]. As in the AB and ABA systems, the BAB ordered gels might align into a mono-domain cubic structure upon application of shear [27,43]. In BAB-networks of PS-PEB-PS micelles, the scattering pattern resembles a twinned body centred cubic morphology with lattice constants of the order of 400Å as shown in Figure 7. Upon cooling, preliminary measurements indicate a transition to

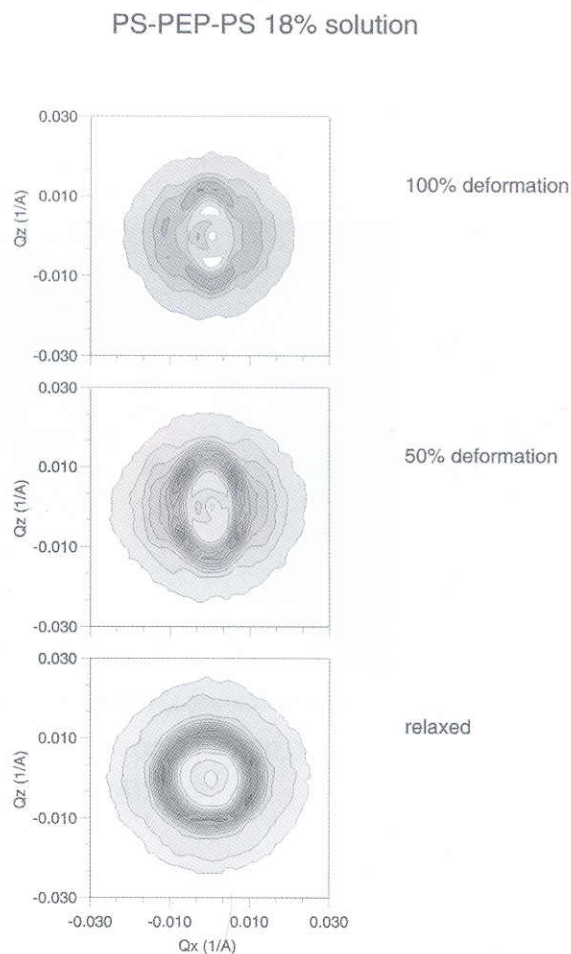


Figure 6: Two dimensional scattering function of PS-PEP-PS when stretched between 2 and 10 times.

another ordered morphology, presumably an fcc-structure.

Conclusions

It is clear from the present review that the field of block-copolymer micelles is an active research field with a large variety of materials. The unique structural characteristics provide novel attractive properties. X-ray and neutron small angle scattering are among the central tools for basic studies of this class of materials.

20% SEBS-1651 in Oil,

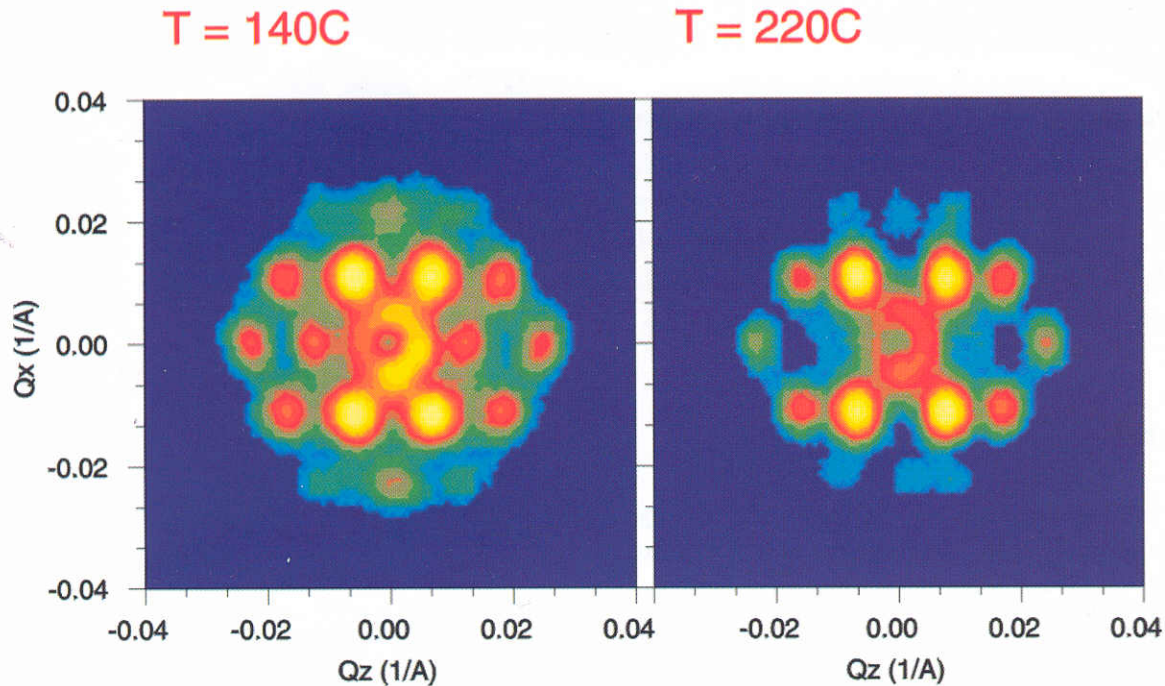


Figure 7: Two-dimensional structure of PS-PEB-PS micellar network structure in two ordered phases: Twinned bcc, and possibly fcc.

References

- [1] Chu, B., *Langmuir* (1995) **11**, 414-421.
- [2] Alexandridis, P. and Hatton, T.A., *Colloids and Surfaces A: Physicochem. Engineering Aspects* (1995) **96**, 1-46.
- [3] Almgren, M., Brown, W. and Hvidt, S., *Colloid Polymer Science* (1995) **273**, 2-15.
- [5] Mortensen, K., *J. Phys.: Condens. Matter* (1996) **8**, A103-A124.
- [6] Alexandridis, P., *Current Opinion in Colloid & Interface Science* (1996) **1**, 490-501.
- [7] Chu, B., Liu, T.B., Wu, C.H., Zhou, Z.K. and Nace, V.M., *Macromolecular Symposia* (1997) **118**, 221-227.
- [8] Hecht, E., Mortensen, K. and Hoffmann, H., *Macromolecules* (1995) **28**, 5465-5476.
- [9] Mortensen, K. and Yeshayahu, T., *Macromolecules* (1995) **28**, 8829-8834.
- [10] Pedersen, J.S. and Gerstenberg, M., *Macromolecules* (1996) **29**, 1363-1365.
- [11] Kinning, D.J. and Thomas, E.L., *Macromolecules* **17**, 1712-1218.
- [12] Brown, W., Schillen, K., Almgren, M., Hvidt, S., and Bahadur, P., *J. Phys. Chem.* (1991) **95**, 1850-1858.
- [13] Wanka, G., Hoffmann, H. and Ulbricht, W., *Colloid Polym. Sci.* (1990) **268**, 101-110.
- [14] Mortensen, K., *Europhys. Lett.* (1992) **19**, 599-604.
- [15] Mortensen, K. and Brown, W., *Macromolecules* (1993) **26**, 4128-4135.
- [16] Mortensen, K. and Pedersen, J.S., *Macromolecules* (1993) **26**, 805-812.
- [17] Mortensen, K., Brown, W. and Norden, B., *Phys. Rev. Letters* (1992) **68**, 2340-2343.
- [18] Mortensen, K., Schwahn, D. and Janssen, S., *Phys. Rev. Letters* **71**, 1728-1831.
- [19] Berret, J.F., Molino, F., Porte, G., Diat, O. and Lindner, P., *Journal of Physics - Condensed Matter* (1996) **8**, 9513-9517.
- [20] Mcconnell, G.A., Lin, M.Y. and Gast, A.P., *Macromolecules* (1995) **28**, 6754-6764.
- [21] Prudhomme, R.K., Wu, G.W. and Schneider D.K., *Langmuir* (1996) **12**, 4651-4659.
- [22] Slawecki, T.M., Glinka, C. and Hammouda, B., *Phys. Rev. E* (1998) **58**, R4084-R4087.
- [23] Molino, F., Berret, J.F., Porte, G., Diat, O. and Lindner, P., *Eu. Phys. J.* (1998) **1**, 59-72.
- [24] Hamley, I.W., Mortensen, K., Yu, G.E. and

Microtubule biopolymers: fibre diffraction and effects of interparticle scattering

W. Bras¹, G.P. Diakun², R.C. Denny², A. Gleeson², C. Ferrero³, Y.K. Levine⁴ and J. F. Díaz⁵

¹ Netherlands Organisation for Scientific research (NWO) DUBBLE CRG/ESRF BP 220 F38043 Grenoble Cedex France

² CLRC Daresbury Laboratory, Daresbury, Warrington, Cheshire WA4 4AD, U.K.

³ European Synchrotron Radiation Facility BP 220 F38043 Grenoble Cedex France

⁴ Utrecht University Molecular Biophysics PO Box 20000 Utrecht Netherlands

⁵ KU Leuven, Laboratory for Chemical and Biological Dynamics, Celestijnenlaan 200 D, Leuven, Belgium

Introduction

Microtubules play several important roles in the cell [1]. They consist of long chains of tubulin protein dimers, called protofilaments, which connect laterally to form a hollow cylindrical structure with an external diameter of approximately 30 nm and a length which can extend to microns. The number of protofilaments can vary, but the predominant number in a normal functioning cell is 13. The persistence length of these polymers is reported to be between 2000 and 5200 μm [2,3], so that for most experiments they can be considered to be a monodisperse rigid rod system with a large polydispersity in the length. In the experiments described here the average length is approximately 5 μm [4] giving an average molecular weight of 10^9 Dalton.

The preparation of hydrated microtubule samples suitable for small angle X-ray fibre diffraction is not trivial. A reasonably successful method has been centrifugation over extended lengths of time (>24 hours) and subsequent rehydration [5]. We have developed a less invasive method using the cooperative effect of the diamagnetic moment of the tubulin dimers in combination with strong magnetic fields to induce orientation on microtubules in diluted solutions. For rigid rod molecules with an axial ratio of 50 - 200 without any constraint applied to them, Flory has predicted that the angular distribution of the long axis would be at most 10.2 -

- Booth, C., *Macromolecules* (1998) **20**, 6958-6963.
- [25] Mortensen, K., Brown, W., Almdal, K., Alami, E. and Jada, A., *Langmuir* (1997) **13**, 3635-3645.
- [26] Mortensen, K., Brown, W. and Jorgensen, E., *Macromolecules* (1994) **27**, 5654-5666.
- [27] Mortensen, K., *Macromolecules* (1997) **30**, 503-507.
- [28] Zhou, Z.K., Chu, B. and Nace, V.M., *Langmuir* (1996) **12**, 5016-5021.
- [29] Zhou, Z.K., Chu, B., Nace, V.M., Yang, Y.W. and Booth, C., *Macromolecules* (1996) **29**, 3663-3664.
- [30] Yang, Y.W., Yang, Z., Zhou, Z.K., Attwood, D. and Booth, C., *Macromolecules* (1996) **29**, 670-680.
- [31] Chu, B. and Wu, G.W., *Macromolecular Symposia* **87**, 55-67.
- [32] Alexandridis, P., Olsson, U. and Lindman, B., *Macromolecules* (1995) **28**, 7700-7710.
- [33] Wu, G.W., Liu, L.Z., Buu, V.B., Chu, B. and Schneider, D.K., *Physica A* (1996) **231**, 73-81.
- [34] Alexandridis, P., Olsson, U. and Lindman, B., *Langmuir* (1996) **12**, 1419-1422.
- [35] Lairez, D., Adam, M., Raspaud, E., Carton, J.P. and Bouchaud, J.P., *Macromolecular Symposia* (1995) **90**, 203-229.
- [36] Raspaud, E., Lairez, D., Adam, M. and Carton, J.P., *Macromolecules* (1996) **29**, 1269-1277; *Macromolecules* (1994) **27**, 2956-2964.
- [37] Mischenko, N., Reynders, K., Koch, M., Mortensen, K., Pedersen, J.S., Fontain, F., Graulus, R. and Reynaers, H., *Macromolecules* (1995) **28**, 2054-2062.
- [38] Mischenko, N., Reynders, K., Scherrenberg, R., Mortensen, K., Fontain, F., Graulus, R. and Reynaers, H., *Macromolecules* (1994) **27**, 2345-2347.
- [39] Laurer, J.H., Bukovnik, R. and Spontak, R.J., *Macromolecules* (1996) **29**, 5760-5762.
- [40] Reynders, K., Mischenko, N., Mortensen, K., Overbergh, N. and Reynaers, H., *Macromolecules* (1995) **28**, 8699-8701.
- [41] Mischenko, N., Reynders, K., Mortensen, K., Overbergh, N. and Reynaers, H., *J. Polym. Science: B. Polym. Phys.* (1996) **34**, 2739-2745.
- [42] Kleppinger, R., Reynders, K., Mischenko, H., Overbergh, N., Koch, M.H.J., Mortensen, K. and Reynaers, H., *Macromolecules* (1997) **30**, 7008-7011.
- [43] Kleppinger, R., Mischenko, H., Reynaers, H., Koch, M.H.J., Almdal, K. and Mortensen, K., *Macromolecules* (1997) **30**, 7012-7014.